Micro and Nano Systems Letters

LETTER

Open Access

Design and performance evaluation of thin-film actuators based on flexible Ni-Co substrates

Suhwan Kim[1], Woojin Kim[2] and Yongdae Kim[1*]

Abstract

This paper proposes a new design of bimorph-type electrothermal actuators based on flexible Ni-Co substrates and describes the results of the finite element method (FEM) simulation and performance evaluation of the actuators. In the design of the actuators, a multilayer structure consisting of an adhesion layer, two insulation layers, and a Pt (platinum) heater layer was formed on the Ni-Co flexible substrate that was patterned in an individual shape. The thin-film actuators proposed in this study could be detached from a Si carrier wafer and adhered to other micro or macrostructural elements. To investigate the temperature distribution and mechanical behavior of the actuators, multiphysics FEM simulations combining electrothermal and static structural analyses were carried out. The actuators were fabricated using conventional microfabrication and electroplating technologies on Si carrier wafer; then, the actuators were peeled off from the carrier wafer using the release process proposed in this paper. After fabricating the actuators, the deflection of their tips was evaluated and compared with that obtained from the FEM simulations.

Keywords: Electrothermal, Actuators, MEMS, Bimorph, Ni-co

Introduction

Advances in planar manufacturing technologies have led to the utilization of new processes and materials for developing a range of innovative microactuators. A microactuator is a device that can generate micro-scale motion in a micro-electromechanical system (MEMS). It consists of functional materials, such as films, fabrics, composites, and inks, and uses layering, patterning, folding, and bonding steps to form complex kinematic structures.

Microactuators are generally categorized into five types [1, 2]: electrostatic, piezoelectric, electromagnetic, shape-memory alloy (SMA), and electrothermal. Electrostatic actuators can generate mechanical motion by changing the stationary electric field in materials [3]. They are faster than electrothermal and SMA actuators and exhibit higher displacements than those of piezoelectric actuators. Therefore, electrostatic actuators are suitable for planar manufacturing and have various applications, such as accelerometers, scanning micro-mirrors, photonics, televisions, and projectors.

Piezoelectric actuators are governed by the principle that stress occurs in materials due to a change in the electrical field applied to the actuators [4]. They are advantageous because of their fast response, high force per unit area, and low power consumption; however, they have limitations such as charge leakage and hysteresis effects.

Electromagnetic actuators [5] can induce motion due to a change in the electrical field. They have several applications owing to their high actuating force, low driving voltage, and large stroke. High power consumption and a requirement for large external magnets are the limitations of electromagnetic actuators.

An SMA is a material that deforms when cooled but returns to its pre-deformed shape when heated. The

*Correspondence: ydkim@kiu.kr
[1] Kyungil University, 38428, 50 Gamasilgil, Hayangeup, Gyeongsan, Gyeongbuk, Republic of Korea
Full list of author information is available at the end of the article

actuating power of SMA actuators is higher than that of other types of actuators; however, they have a drawback of being difficult to miniaturize [6].

Electrothermal actuation is based on the balance between the thermal energy generated by an electrical current and the heat dissipated through the environment or the substrate. Conventionally, there are three types of electrothermal actuators: hot-and-cold-arm, chevron, and bimorph. Guckel et al. [7] proposed the hot-and-cold-arm actuator. Hot-and-cold-arm [8, 9] and chevron-type actuators [10–12] commonly use homogeneous materials and consist of multiple beams. Bimorph-type electrothermal actuators rely on the thermal expansion factor and operate by utilizing the difference in the coefficient of thermal expansion (CTE) of structural materials. Such actuators are easy to manufacture because they do not require processing or special materials. They are useful in low power and very large-scale operations.

In this study, a new design for bimorph-type electrothermal actuators was proposed. The proposed actuators possessed a flexible structure that consisted of a Pt (platinum) heater layer and two SiO_2 and Si_3N_4 insulation layers on a Ni-Co thin film. Electricity was applied to the Pt heater to generate heat, which caused the thin film to bend owing to the difference in the CTE between the Ni-Co film and the insulation layers. While contemporary electrothermal actuators are embedded in the Si substrate, the proposed Ni-Co-based actuators can detach from the Si carrier wafer and adhere to other micro or macro structures, including curved surfaces. Therefore, they have applications in various electro-mechanical systems. Figure 1 shows an example of applying the thin film electrothermal actuators to a micromirror system. The micromirror system can be implemented by assembling the mirror sheet to the support structure; the mirror sheet consists of the electrothermal actuator, electrode pads, and mirror formed on the Ni-Co flexible substrate. Supplying electrical power to the mirror, the electrothermal actuators are deformed, allowing the micromirror to rotate. The design example of the micromirror system shows that the planar structure separated from the Si carrier wafer can be simply transformed into the 3D structure.

Prior to fabrication of the electrothermal actuators, the temperature distribution and mechanical behavior of the actuators were estimated using multiphysics simulations that combined electrothermal and static structural analyses by using a finite element method (FEM) tool. Then, the fabrication process of the actuators based on a Ni-Co flexible substrate was established. The fabrication of flexible actuators with complex shapes and thicknesses of several micrometers was achieved using a combination of the micro-fabrication and conventional electroplating technologies of Ni-Co [13]. After fabricating the

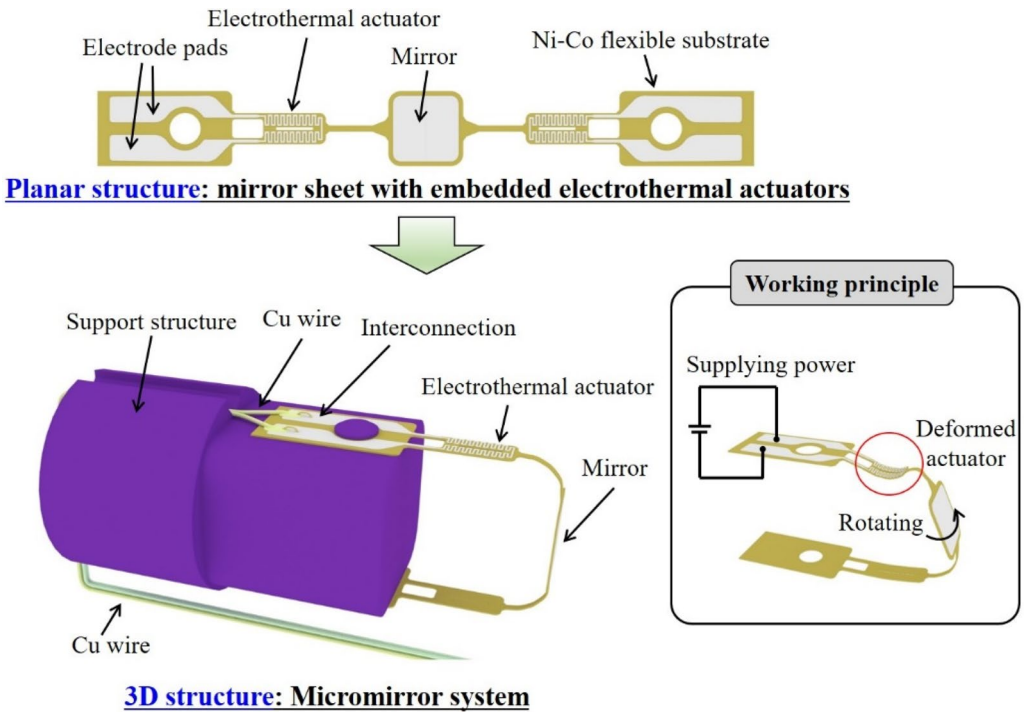

Fig. 1 Schematic of a micromirror system operated by thin film electrothermal actuators

actuators, the temperature distribution and deflection of their tips was evaluated and compared with that obtained from the FEM simulations.

Design and FEM simulation

A schematic of an electrothermal actuator based on a Ni-Co flexible substrate is shown in Fig. 2a. In this study, the bimorph beam was a cantilever comprising a Ni-Co substrate along with the adhesion, insulation, and heater layers. Thermal bimorph actuation occurred due to the difference in the CTEs of the materials of the Ni-Co thin film and the SiO_2 and Si_3N_4 insulation layers. Upon actuation, voltage was supplied to the Pt heaters, and the Joule effect heated up the bimorph beams. Since Ni-Co has a higher CTE than that of SiO_2 and Si_3N_4, the bimorph beam bent upward. The length and width of the actuating parts were 4.1 and 1 mm, respectively. A Pt heater, with a thickness of 40 μm, was embedded throughout the surface of the bimorph beams to ensure uniform and efficient heating. The bridge structures between the actuating and the support parts of the cantilever ensured effective thermal isolation.

Figure 2b shows the multilayer structure of the actuator. There is a Ti/Pt layer at the top, followed by the Si_3N_4 and SiO_2 insulation layers, an adhesion-promoting layer of Ti, and a bottom substrate layer of Ni-Co. The thicknesses of the Pt, Si_3N_4, SiO_2, and Ti layers, and the Ni-Co thin film were 0.2, 0.3, 0.7, 20, and 5 μm, respectively.

To examine the temperature distribution and mechanical behavior of the actuator, multiphysics simulations combining electrothermal and static structural analyses were performed using an FEM tool ANSYS. Figure 3

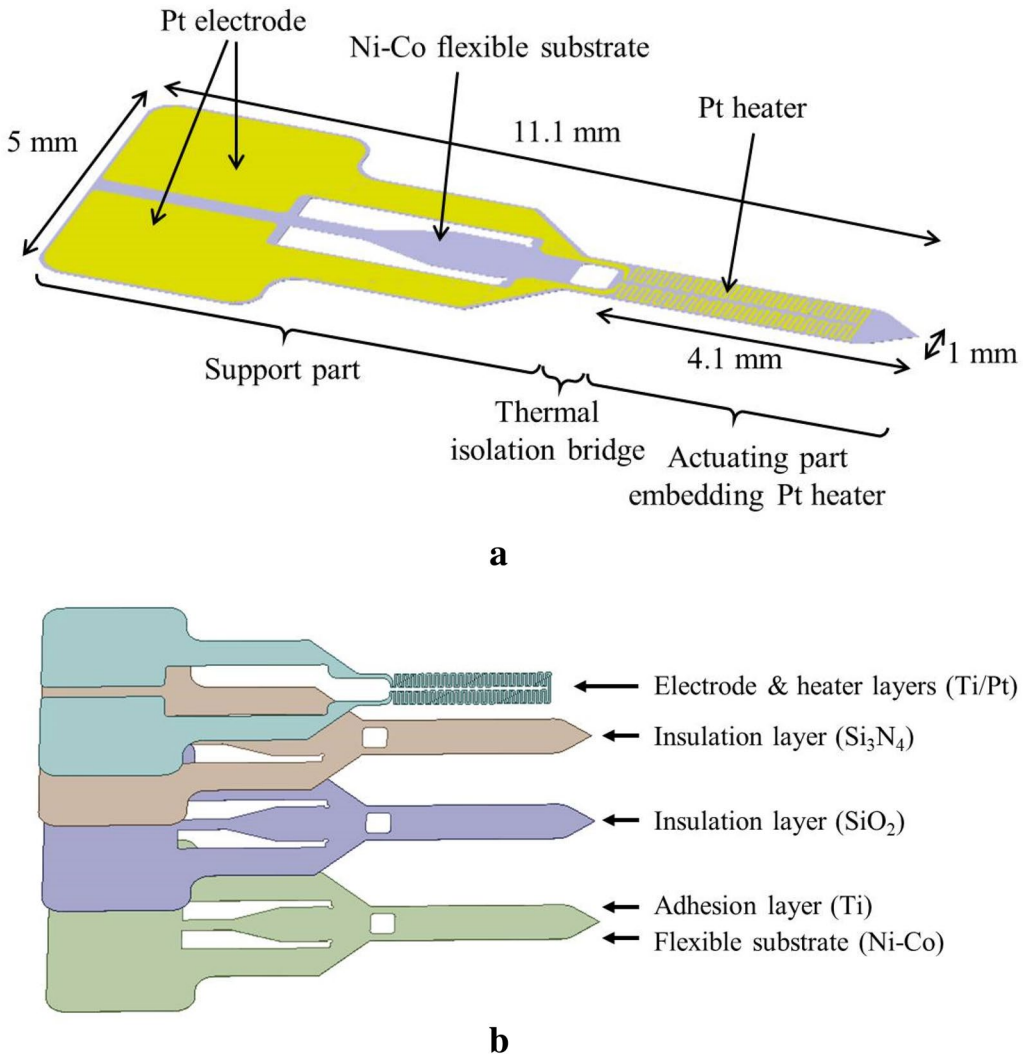

Fig. 2 **a** Schematic of a bimorph-type electrothermal actuator based on a Ni-Co flexible substrate and **b** layer structure of the actuator

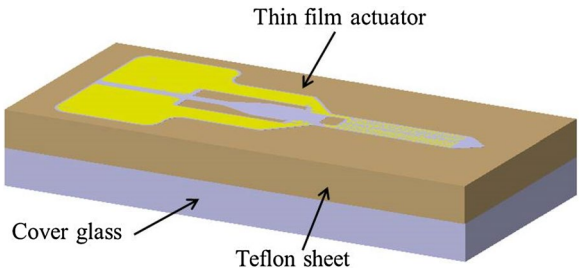

Fig. 3. 3D model for FEM simulation

shows the 3D model of the FEM simulation; the actuator was attached to a base plate consisting of a Teflon sheet and cover glass. The simulation was performed by mechanically fixing the support part of the actuator while all the other boundaries were free to move.

Heat was generated when DC voltage was applied across the Pt resistor. In the steady state, this heat dissipated into the atmosphere and the base plate through convection and conduction, respectively. The temperature of the actuator was determined by the amount of heat loss. The surface temperature of the actuator was calculated using the electrothermal simulation module of ANSYS. This data were then used to simulate the thermo-mechanical deformation that occurred due to the difference in the CTE. The physical properties of the materials used for the FEM simulation are summarized in Table 1. The atmospheric temperature was set to 22 °C to replicate the experimental conditions.

Fabrication

Figure 4 shows the fabrication process of the electrothermal actuator. A 1 μm thick layer of SiO_2 was deposited on an Si wafer using low-pressure chemical vapor deposition (CVD) to ensure electrical isolation from the Si carrier wafer. A 200 Å thick Ti layer and a 200 nm thick Cu layer were then deposited by sputtering to form a seed layer for Ni-Co plating. A photoresist (PR) was coated

Table 1 Properties of the materials used for FEM simulation

Property	Ni-Co	Platinum	Silicon dioxide	Silicon nitride
Density (kg/m^3)	8913	21,450	2170	2370
Thermal expansion (ppm/K)	17.8	9	0.55	1.4
Young's modulus (GPa)	320	154	66	166
Poisson's ratio	0.31	0.39	0.15	0.23
Tensile yield strength (MPa)	1500	120	450	60
Thermal conductivity (W/m·K)	55.35	70	1.3	10
Resistivity (Ω·cm)	1.33×10^{-5}	1.04×10^{-5}	–	–

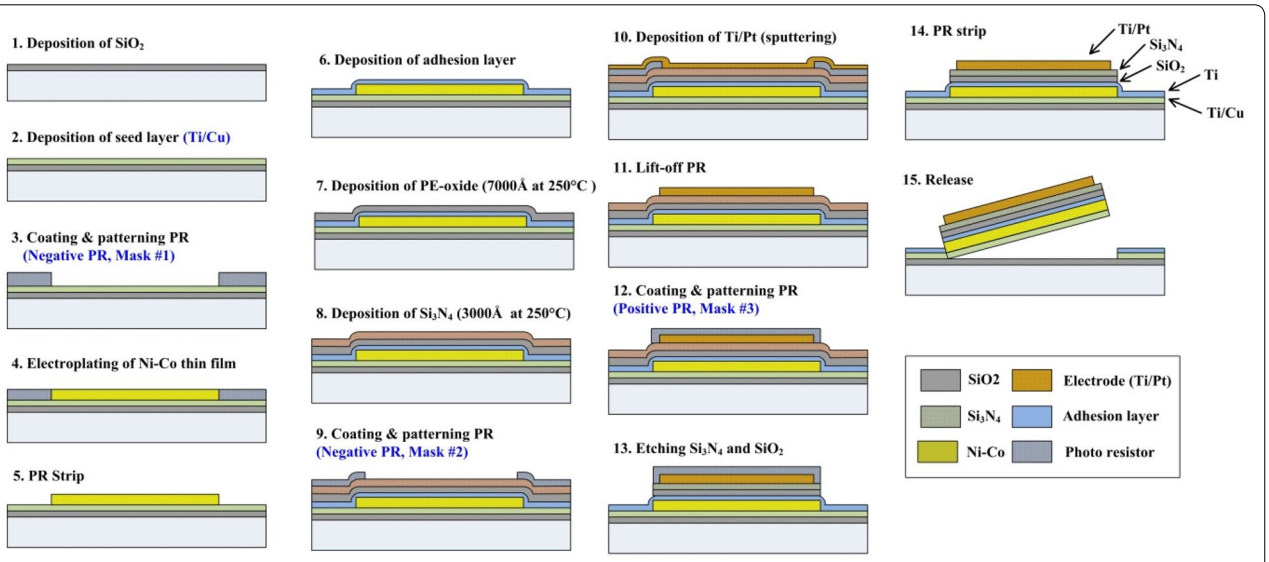

Fig. 4 Fabrication process of the thin-film actuator

and patterned to form a plating frame. Since the PR-coated region was not electroplated, the desired shape of the Ni-Co thin film could be obtained. A 5 μm thick Ni-Co thin film was plated using electroplating equipment with a current density of 1 A per square decimeter (ASD). After removing the PR, the Ti/Cu/Ni-Co thin film remained on the Si carrier wafer on which SiO_2 had been deposited (Fig. 4(5)). The adhesion-improving 200 Å thick Ti layer was then deposited on the Ni-Co film. Subsequently, the 700 nm thick SiO_2 and 300 nm thick Si_3N_4 insulation layers were deposited using plasma-enhanced CVD at 250 °C. The PR was coated and patterned, after which a 40 nm thick Ti adhesion layer and a 200 nm thick Pt layer were deposited by sputtering. Pt metallization of individual shapes can be fabricated by lifting off the PR to form a Pt heater and electrodes. Finally, the PR was coated and patterned, which was followed by wet etching of SiO_2 and Si_3N_4 to produce a thin-film actuator with the desired shape. In this actuator, the adhesion, insulation, and Ti/Pt metallization layers were formed on the Ni-Co metallic thin film. Afterward, the actuators based on the Ni-Co metallic substrate were peeled off from the Si carrier wafer.

Figure 5 shows the release process of the actuator where the release tag was formed at one end of the actuator. In the release process, the edge of the release tag was separated by scribing with a tweezer (Fig. 5(1)). The actuator could then be peeled off from the wafer by pulling the release tag with the tweezer (Fig. 5(2–4)). The 6 μm thick actuator exhibited flexibility and possessed high mechanical strength owing to the high elastic modulus and yield strength of the Ni-Co substrate, as summarized in Table 1. Figure 6 shows the actuator after it was peeled off from the Si carrier wafer. The release tag that was damaged during the release process was separated by cutting it with scissors.

Scanning electron microscopy (SEM) (SU8230, Hitachi) was used to examine the cross-sectional structure and adhesion strength of the actuators, after using precision medical scissors to cut through all the layers of the actuator, from the Ni-Co substrate to the Pt metallization layer. The SEM image (Fig. 7) showed no delamination, which indicated the strong adhesion strength between each layer.

Results and discussion

In this study, the displacement of the actuator tip was measured and compared with that obtained from the simulation results. In the FEM simulation, voltages of 1–14 V were applied to the Pt heater. The electric power supplied to the actuator was calculated as follows:

$$P = \frac{V^2}{R} \tag{1}$$

where P, V, and R indicate the electric power, voltage, and resistance of the Pt heater, respectively. The resistance of the Pt heater changed with temperature; this property is common to almost all conductors. Therefore, the electric power corresponding to voltages of 1–14 V ranged from 0.0015–0.2422 W. The temperature distribution of the actuator was calculated from the heat generated due to Joule heating and the heat loss through convection

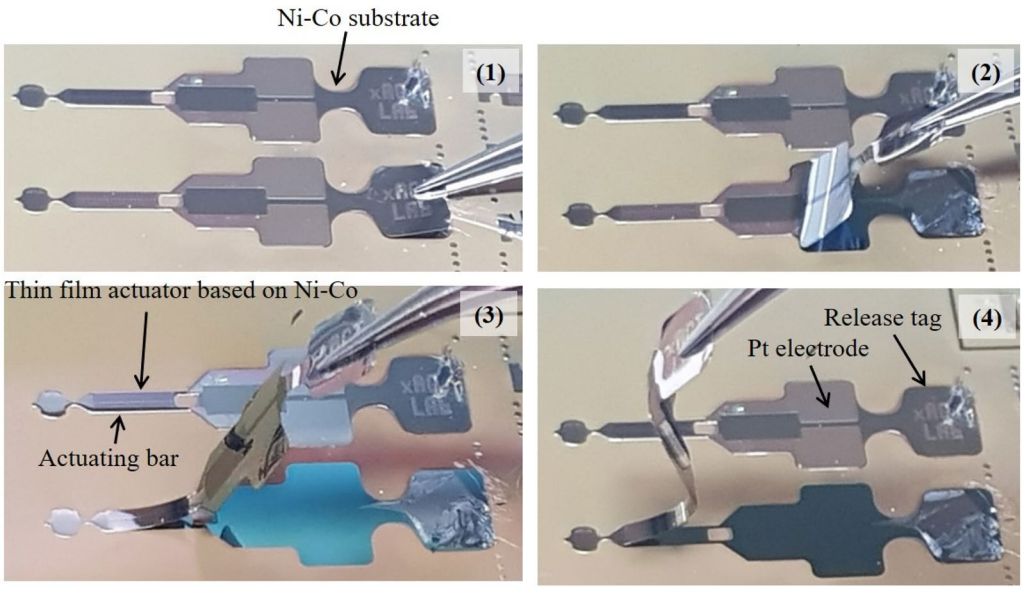

Fig. 5 Release process of the thin-film actuator

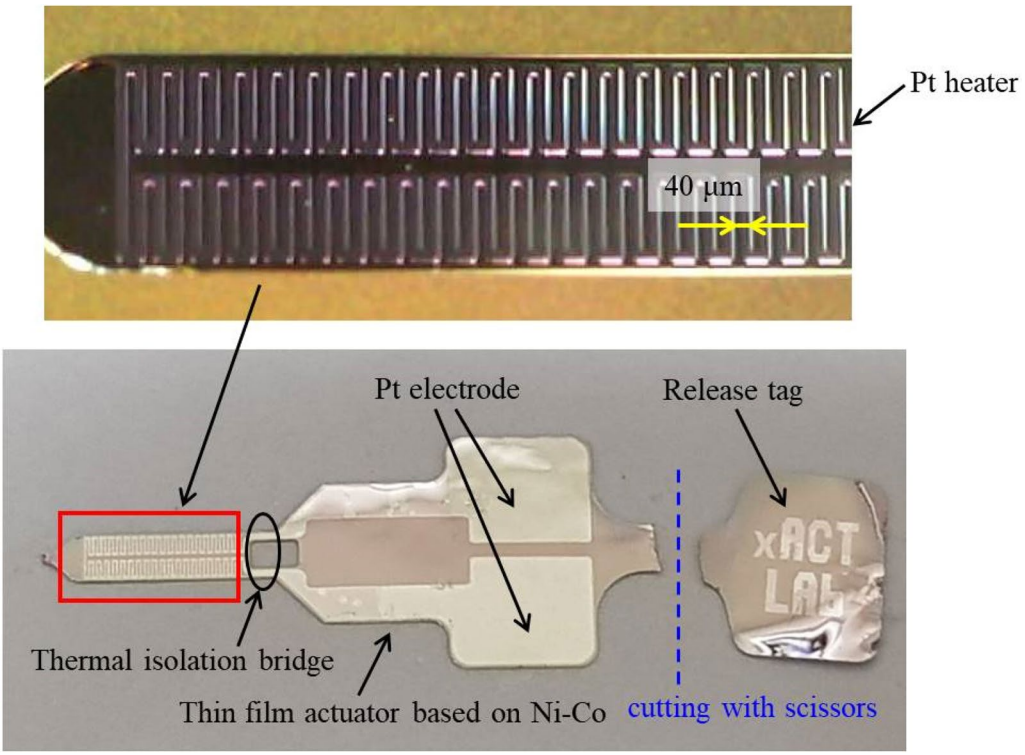

Fig. 6 Fabricated thin-film actuator

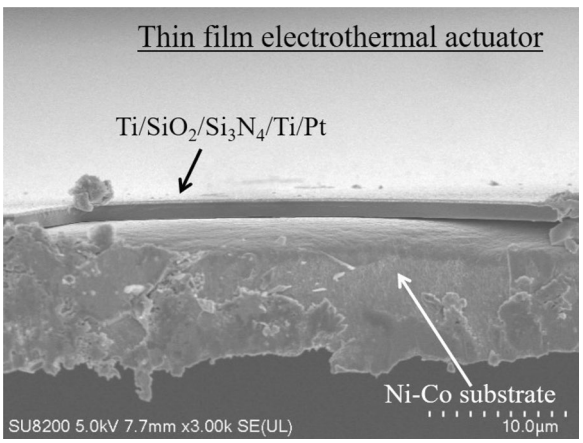

Fig. 7 SEM image of the cross-section of the thin-film actuator

and conduction to the atmosphere and the base plate, respectively. In the FEM simulation, the temperature of the actuator was calculated using the heat generated, the heat loss, and the change in the aforementioned resistance of the Pt heater.

Figures 8 and 9 show the FEM simulation results of the temperature distribution and the deformation of the actuator at 2 and 14 V, respectively. The temperature of the cantilever, on which the Pt heater was formed, was uniformly distributed but rapidly decreased at the periphery of the support part due to the heat loss to the support part.

Figure 10 shows the temperature of the Pt heater as a function of the electric power. The temperature increased exponentially with the power because the convective heat transfer coefficient changed exponentially with increasing power. The maximum temperature of the Pt heater reached approximately 149 °C at a power of 0.2422 W.

The FEM simulation results of the deformations showed that the tip of the cantilever was deflected upward because the CTEs of the SiO_2 and Si_3N_4 insulation layers were lower than that of the Ni-Co flexible substrate. The vertical displacement of the actuator tip reached 1.44 mm.

Figure 11 shows a schematic of the equipment used to test the actuator performance. The actuator was attached to a base plate consisting of a Teflon sheet and cover glass as shown in Fig. 3. Fluorine in the Teflon is an extremely

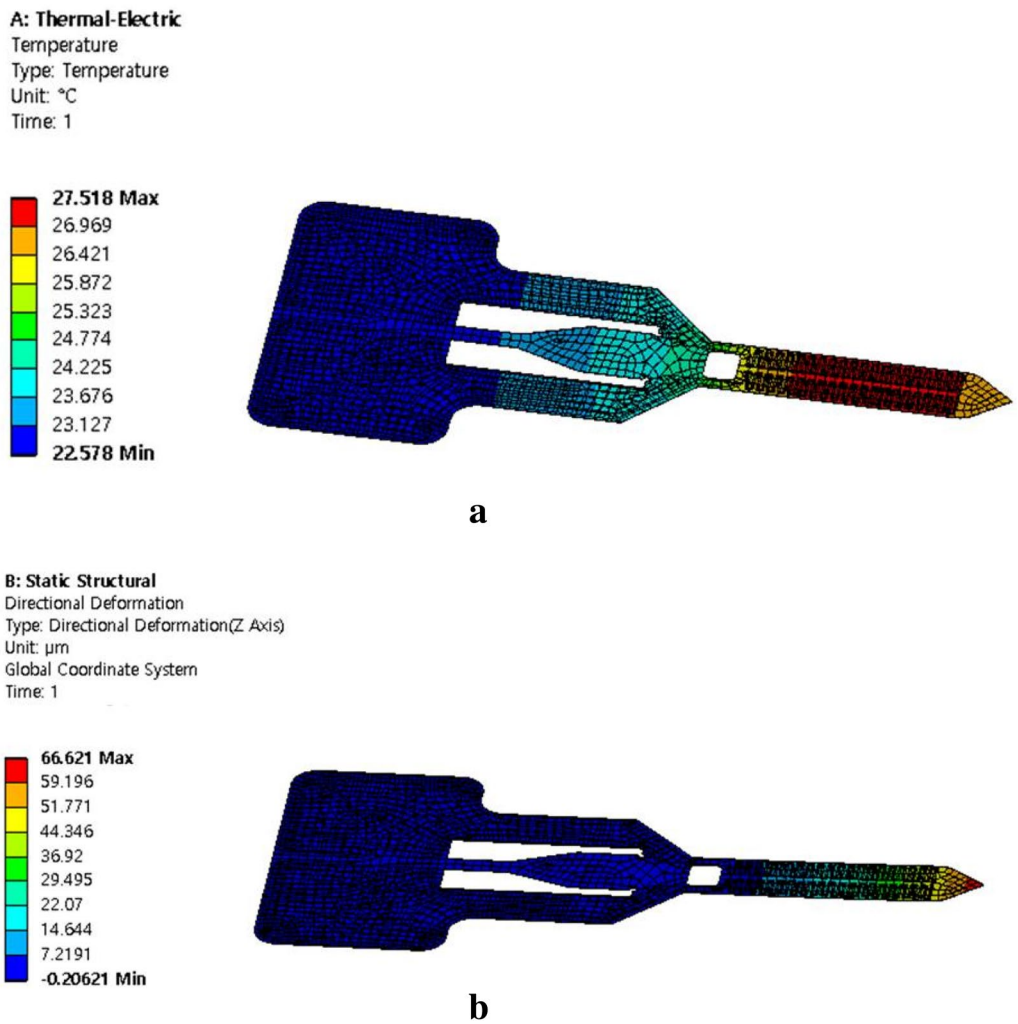

Fig. 8 FEM simulation results at 2 V; **a** temperature distribution and **b** deformation

electronegative element, indicating a weak van der Waals force between the Ni-Co substrate and the Teflon sheet. Therefore, the Teflon sheet was used to prevent the actuator from sticking to the base plate. Voltages of 1–14 V were supplied (OPE-303QI, ODA) to the Pt heater, and the change in deflection was measured with a CCD microscope (AM7013MZT, Dino-Lite). The deflection of the actuator tip was accurately measured using image-processing software to compare the scales of the precision ruler.

Figure 12 shows the acquired images of the actuator and the ruler. At 4 V, corresponding to a power of 0.0236 W, the actuator began to bend upward; at 14 V, the deflection height reached 1.083 mm. Initially, the actuator was concave downward due to the residual stress generated in each layer during the deposition process. Therefore, power of 0.0236 W was required to flatten the warped actuator; this was confirmed by plotting the deflection height of the actuator tip as a function of the electric power (Fig. 13). The solid rhombi and circles in Fig. 13 indicate the experimental and simulation data, respectively. The experimental data showed that the displacement of the tip was unchanged when the power was less than 0.0135 W and increased linearly thereafter. The blank rhombi represent the results that shifted the experimental data by − 0.0135 W in the x-direction to compensate for the power required to flatten the actuator. The simulation data and the compensated experimental data were confirmed to be similar. We estimated the deformation characteristics of the electrothermal actuator based on an Ni-Co flexible substrate from the experimental data and the simulation results.

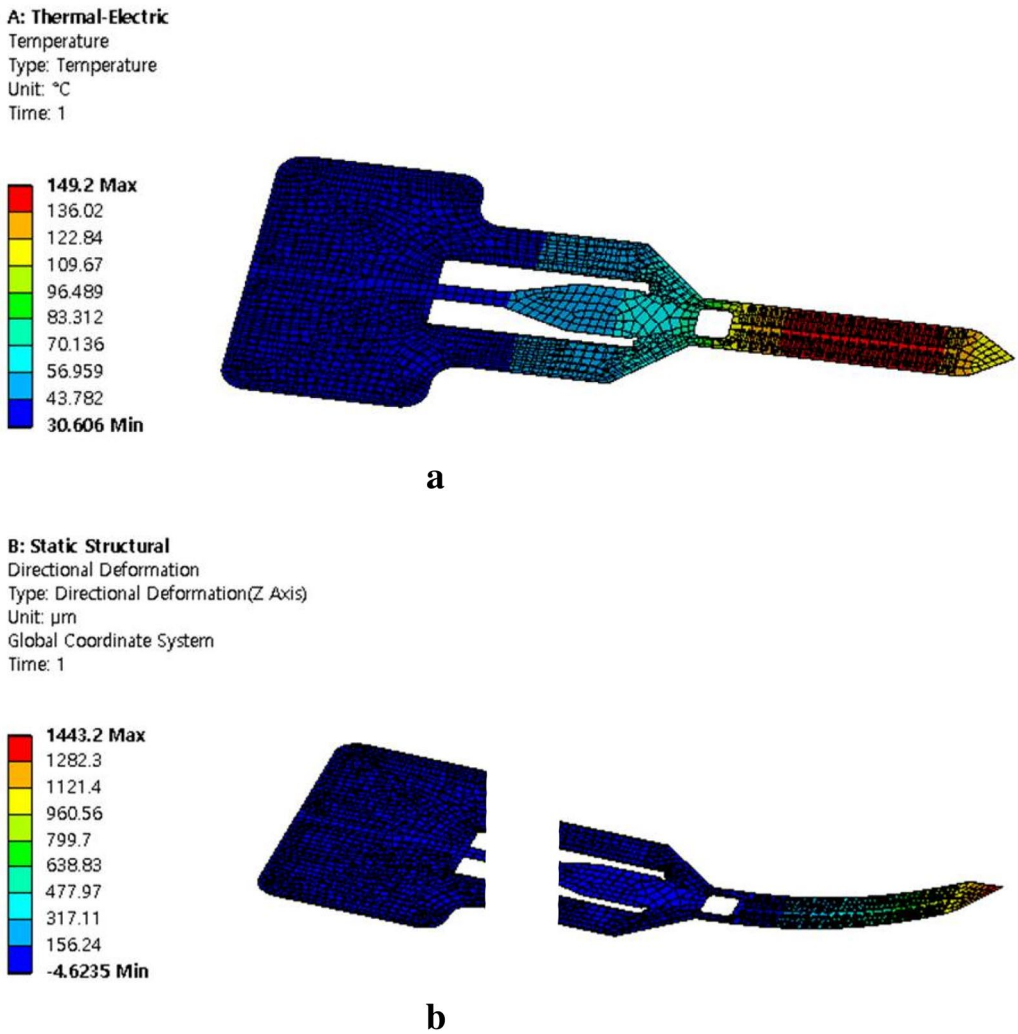

Fig. 9 FEM simulation results at 14 V; **a** temperature distribution and **b** deformation

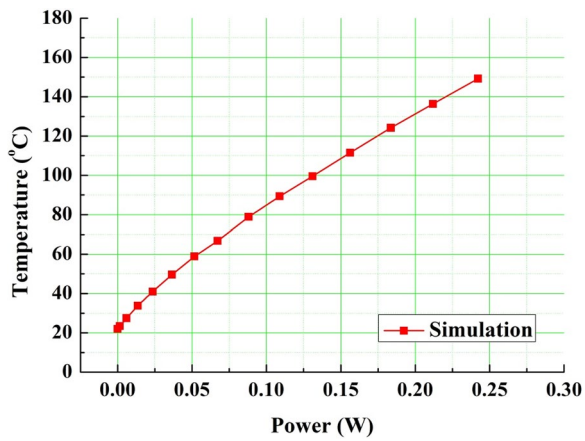

Fig. 10 Temperature of the Pt heater as a function of electric power

Conclusion

In this study, the design of a bimorph-type electrothermal actuator was proposed. FEM simulations and experiments were used to evaluate its deflection characteristics. The proposed actuator had a multilayered structure, where a Pt heater, SiO_2 and Si_3N_4 insulation layers, and adhesion-promoting layers were deposited on a Ni-Co thin film. The heat generated from the Pt heater caused the thin film to bend because of the difference in the CTEs of the Ni-Co film and the insulation layers. The proposed Ni-Co-based actuator detached from the Si substrate without any damage and adhered to other structures. This shows that such actuators can be applied to various electro-mechanical devices, such as micromirrors, origami robots, and mechanical metamaterial actuators.

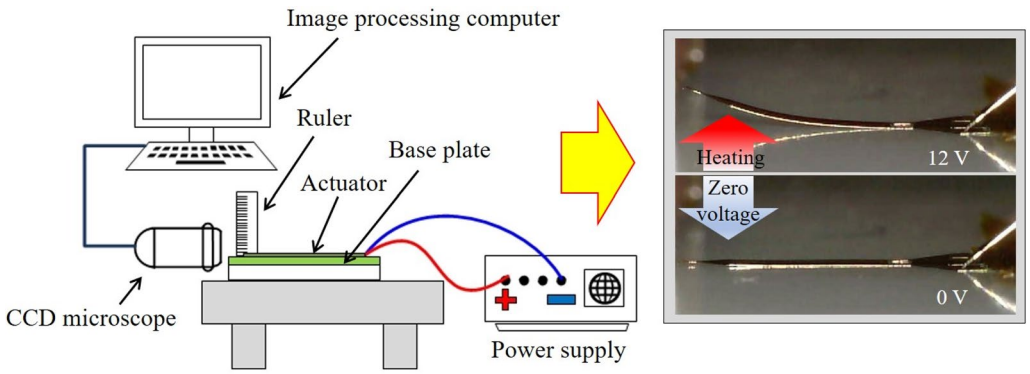

Fig. 11 Experimental setup for testing the performance of the thin-film actuator

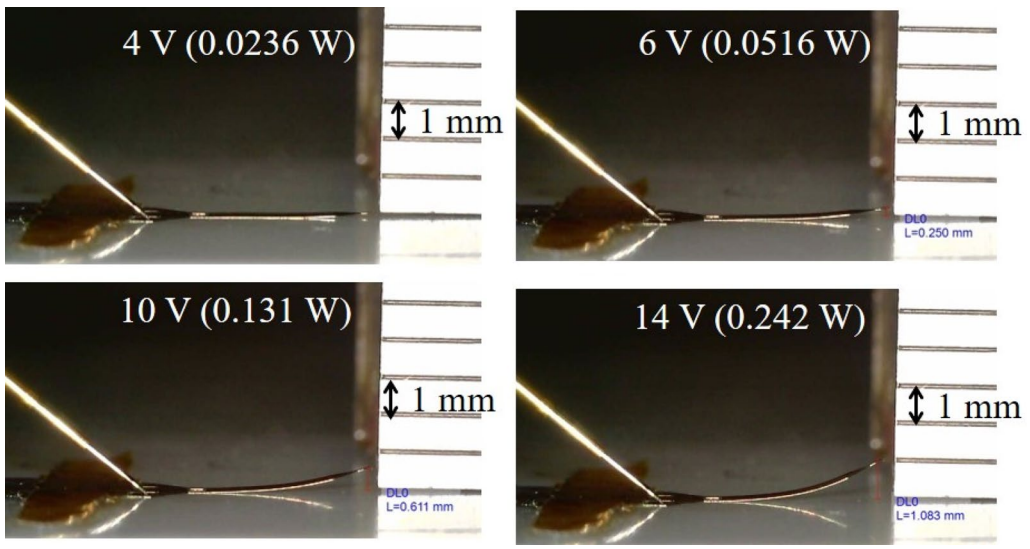

Fig. 12 Operational images of the thin-film actuator at different input voltages

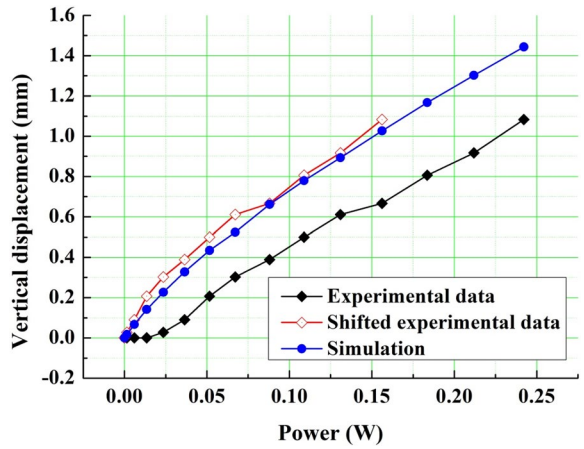

Fig. 13 Vertical displacement of the actuator tip as a function of input power

In the experimental results, the deformation did not occur until a power of approximately 0.0135 W was supplied; thereafter, the upward deflection of the actuator tip increased linearly as the power supply increased, which was confirmed by the simulation results. The deflection height of the tip reached 1.083 mm at 14 V.

Acknowledgements
We thanks to members of our laboratory (xACT Lab.) for sincere comments on this research.

Authors' contributions
SK conducted the main experiment. WK advised FEM simulation method. YK supervised the project. All authors read and approved the final manuscript.

Funding
This study was conducted with the support of the Korea Science and Engineering Foundation through the funding of the Ministry of Education, Science, and Technology in 2020 (NRF-2019R1F1A1060772).

Availability of data and materials
All data generated or analyzed during this study are included in this published article.

Competing interests
The authors declare no competing interests (both financial and non-financial).

Author details
[1] Kyungil University, 38428, 50 Gamasilgil, Hayangeup, Gyeongsan, Gyeongbuk, Republic of Korea. [2] Safety System R&D Group, Korea Institute of Industrial Technology, Daegu, Republic of Korea.

Received: 1 July 2020 Accepted: 1 November 2020
Published online: 13 November 2020

References

1. Potekhina A, Wang C (2019) Review of electrothermal actuators and applications. Actuators 8:69
2. Yang S, Xu Q (2017) A review on actuation and sensing techniques for MEMS-based microgrippers. J Micro Bio Robot 13:1–14
3. Conrad H, Schenk H, Kaiser B et al (2015) A small-gap electrostatic microactuator for large deflections. Nat Commun 6:10078
4. Adriaens HJMTS, De Koning WL, Banning R (2000) Modeling piezoelectric actuators. IEEE-ASME T Mech 5(4):331–341
5. Xingdong L, Weiwei W, Xu M et al (2015) A novel MEMS electromagnetic actuator with large displacement. Sensor, Actuat, A-Phys 221:22–28
6. Ikuta K (1990) Micro/miniature shape memory alloy actuator. Proc IEEE Int Conf Robot Autom 3:2156–2161
7. Guckel H, Klein J, Christenson T, Skrobis K, Laudon M, Lovell EG (1992) Thermo-magnetic metal flexure actuators. In: Proceedings of the Technical Digest IEEE Solid-State Sensor and Actuator Workshop, Hilton Head Island, SC, USA, 22–25 June 1992, pp 73–75
8. Hickey R, Kujath M, Hubbard T (2002) Heat transfer analysis and optimization of two-beam micro-electro-mechanical thermal actuators. J Vac Sci Technol A 20:971–974
9. Chen WC, Chu CC, Hsieh J et al (2003) A reliable single-layer out-of-plane micromachined thermal actuator. Sensor Actuat A-Phys 103:48–58
10. Enikov ET, Kedar SS, Lazarov KV (2005) Analytical model for analysis and design of V-shaped thermal microactuators. J Microelectromech S 14:788–798
11. Kwan AMH, Song S, Lu X et al (2012) Improved designs for an electrothermal in-plane microactuator. J Microelectromech S 21:586–595
12. Luo JK, Flewitt AJ, Spearing SM et al (2005) Comparison of microtweezers based on three lateral thermal actuator configurations. J Micromech Microeng 15:1294–1302
13. Kim J, Kim W, Kim Y et al (2020) Fabrication and performance evaluation of Pt strain gauges formed on ni-co flexible structures for applicable to micro force sensors. Trans Korean Soc Mech Eng B 44(2):135–141

Publisher's Note